PCCP

RSC Publishing

PAPER

View Article Online
View Journal | View Issue

Cite this: *Phys. Chem. Chem. Phys.*, 2013, **15**, 15185

Tuning the dissolution kinetics of wollastonite *via* chelating agents for CO_2 sequestration with integrated synthesis of precipitated calcium carbonates

Huangjing Zhao,†[a] Youngjune Park,†[a] Dong Hyun Lee[b] and Ah-Hyung Alissa Park*[a]

Received 13th June 2013,
Accepted 26th June 2013

DOI: 10.1039/c3cp52459k

www.rsc.org/pccp

Carbon mineralization has recently received much attention as one of the most promising options for CO_2 sequestration. The engineered weathering of silicate minerals as a means of permanent carbon storage has unique advantages such as the abundance of naturally occurring calcium and magnesium-bearing minerals and the formation of environmentally-benign and geologically stable solids *via* a thermodynamically favored carbonation reaction. However, several challenges need to be overcome to successfully deploy carbon mineralization on a large scale. In particular, the acceleration of the rate-limiting mineral dissolution step along with process optimization is essential to ensure the economic feasibility of the proposed carbon storage technology. In this study, the effect of various types of chelating agents on the dissolution rate of calcium-bearing silicate mineral, wollastonite, was explored to accelerate its weathering rate. It was found that chelating agents such as acetic acid and gluconic acid significantly improved the dissolution kinetics of wollastonite even at a much diluted concentration of 0.006 M by complexing with calcium in the mineral matrix. Calcium extracted from wollastonite was then reacted with a carbonate solution to form precipitated calcium carbonate (PCC), while tuning the particle size and the morphological structure of PCC to mimic commercially available PCC-based filler materials.

Introduction

The reduction and stabilization of the atmospheric CO_2 concentration is currently one of the most challenging problems being investigated by researchers in the energy and environmental research areas.[1,2] Efforts to develop renewable energy sources and improve the efficiency of energy production and utilization are underway to reduce anthropogenic CO_2 emissions. However, given the rapidly rising global demand for energy and increasing consumption of fossil fuels, CO_2 capture, utilization and storage (CCUS) technologies are necessary to curb the atmospheric CO_2 concentration.[3] Various schemes have been proposed and developed for technologically and economically feasible CCUS.[4,5] Currently, the research and development of ocean sequestration has nearly stopped in most regions and the geological storage of CO_2 has been considered as the most economical method for carbon sequestration, while CO_2 storage by forming mineral carbonates is a relatively new and less explored carbon storage scheme.[6–13]

Since the introduction of the conceptual mineral sequestration as an option for CCUS by Seifritz in 1990,[10] detailed design of such reaction schemes has been proposed,[14] and *in situ* mineral carbonation has also been investigated as a positive fate of CO_2 injected in geologic formations.[15] The direct carbonation of earth abundant Mg-bearing silicate minerals such as olivine and serpentine was first attempted in a gas–solid process under high pressure and high temperature conditions (*i.e.*, 500 °C and 340 bar) by Butt *et al.*, but showing a very slow conversion rate.[16] Lackner *et al.* proposed an indirect mineral carbonation process to produce a more reactive form of magnesium ($MgCl_2$) *via* a multi-step approach.[17] While the indirect processes offered relatively fast reaction kinetics and better product quality, the reaction pathways were too complex and energy intensive.[18,19] Since then a direct mineral carbonation scheme in aqueous solutions was developed by O'Connor *et al.*,[20–22] and significant attempts have been made *via* pretreatment of Mg-bearing minerals, for example, heat treatment of hydrous magnesium silicate and *ex situ* attrition grinding of olivine. It has also been identified that the process parameters such as pH, temperature, pressure, and particle size distribution significantly affect each reaction kinetics of the mineral carbonation process.[23,24]

[a] *Department of Earth and Environmental Engineering, Department of Chemical Engineering, and Lenfest Center for Sustainable Energy, Columbia University, New York, NY 10027, USA. E-mail: ap2622@columbia.edu; Fax: +1 212-854-7081; Tel: +1 212-854-8989*

[b] *Department of Chemical Engineering, Sungkyunkwan University, 300 Chunchun, Jangan, Suwon Gyeonggi 440-746, Republic of Korea*

† Authors with equal contributions.

More recently, the extraction of Mg or Ca from silicate minerals using chemical additives such as salts, acids, alkali solutions and ligands has been proposed[25–28] and Park and Fan investigated the effects of the chelating agents and the *in situ* physical activation on the serpentine dissolution along with a pH swing scheme to further enhance mineral carbonation.[26] The pH swing technology allows the production of high purity iron oxide and $MgCO_3$ as value-added products, which could potentially reduce the overall cost of carbon sequestration. The effects of weak organic acids and other chemical additives on the enhancement of the mineral dissolution kinetics were also reported.[29–32]

The selection of minerals for either *in situ* or *ex situ* carbon mineralization largely depends on the regional geologic conditions and the reactivity of the minerals as well as potential utilization of produced solids. The theoretical CO_2 binding capacity (R_{CO_2}) for serpentine is 2.1 (ton-mineral/ton-CO_2), whereas R_{CO_2} of wollastonite is 2.6 (ton-mineral/ton-CO_2).[33,34] Thus, less serpentine is needed compared to wollastonite to store the same amount of CO_2. However, in terms of reactivity Ca-based silicate materials have great potential and the utilization of precipitated calcium carbonate (PCC) would be relatively straightforward since PCC is already widely used as important commodity material (*e.g.*, filler materials in paper, paints, and plastics/rubber industries).[35]

CO_2 mineralization using Ca-bearing minerals could be a plausible option in specific areas where Ca-bearing silicates are largely deposited. The world reserves of wollastonite are estimated to exceed 90 million tons (with the reported maximum estimation of 270 million tons),[36] with large reserves in China, Finland, India, Mexico, Spain, and the United States.[37] New York State, for example, which has one of the largest deposits of wollastonite in the United States is a suitable place to adapt CO_2 mineralization using Ca-bearing minerals as a CO_2 storage option. Moreover, the technologies developed for enhancing carbonation of Ca-bearing minerals can also be applied to the industrial wastes with similar chemistry, such as steel slag and cement kiln dust.[38–41]

In this study, the effect of various types of chelating agents on the dissolution of wollastonite was investigated to accelerate and optimize the weathering kinetics of Ca-bearing silicate minerals. The aqueous carbon mineralization reaction scheme presented here also includes the subsequent formation of PCC as a result of CO_2 reaction with the extracted calcium ions. By controlling the reaction temperature and pH, the particle size distribution and the morphology of the synthesized PCC were tailored for various utilization options.

Experimental section

Materials

Wollastonite was procured from R.T. Vanderbilt Co., Inc. (Norwalk, CT). In order to control the particle size for the dissolution kinetic studies, the raw mineral sample was ground and sieved to prepare homogenous mineral samples with the mean particle size of 108.59 μm. The particle size distribution and the crystalline structure of the prepared sample was obtained *via* the laser diffraction measurement (LS™ 13 320 MW, Beckman Coulter, Inc., Brea, CA) and an X-ray diffractometer (XRG 3000, Inel Inc., Stratham, NH), respectively. The powder X-ray diffraction (XRD) patterns were obtained in the 2θ range of 20–60° at room temperature, using CuKα radiation (λ = 1.5406 Å). In order to analyze the crystalline structure and the corresponding composition of the mineral sample using the XRD patterns, a Rietveld refinement method was used *via* MAUD (Material Analysis Using Diffraction) package.[42]

Mineral dissolution

Various chelating agents were selected based on their stability constants forming complexes with Ca in the aqueous phase (Table 1): acetic acid (CH_3COOH), nitrilotriacetic acid (NTA) ($C_6H_9NO_6$), picolinic acid ($C_6H_5NO_2$), iminodiacetic acid (IDA) ($HN(CH_2CO_2H)_2$), ethylenediaminetetraacetic acid (EDTA) ($C_{10}H_{16}N_2O_8$), gluconic acid ($C_6H_{12}O_7$), phthalic acid ($C_8H_6O_4$), citric acid ($C_6H_8O_7$), ascorbic acid ($C_6H_8O_6$), glutamic acid ($C_5H_9NO_4$), and oxalic acid ($C_2H_2O_4$). All chelating agents were supplied by Sigma-Aldrich Co. LLC (St. Louis, MO). A custom-made differential bed reactor shown in Fig. 1 was used to explore the fast surface dissolution kinetics for each selected chelating agent. In a differential bed reactor, the mineral sample would always be in contact with fresh solvent and by design the thickness of the mineral sample layer is thin enough to achieve negligible pH gradient along the direction of the solvent flow. Thus, there was no need to buffer the solvent for the differential bed experiments. If the same experiments were performed with a batch system without buffers, the proton concentration in the solvent would have significantly changed and it would be difficult to isolate the effect of chelating agents on the wollastonite dissolution.

A syringe with a solvent capacity of 60 ml was used, coupled with a syringe pump (NE-1000, New Ear Pump System Inc., Farmingdale, NY). The solvents containing chelating agents were prepared at various concentrations: 0.006 M for monoprotic acids (*i.e.*, acetic acid, picolinic acid, and gluconic acid), 0.003 M for diprotic acid (*i.e.*, IDA, phthalic acid, ascorbic acid, glutamic acid, and oxalic acid), 0.002 M for triprotic acid (*i.e.*, NTA and citric acid), and 0.0015 M for tetraprotic acid (*i.e.*, EDTA).

Table 1 Properties of various chelating agents (β = stability constant)

Ligands	Molecular formula	Complex	$\log\beta$
Ascorbate	$C_6H_6O_6^{2-}$	CaL	0.19
Acetate	$C_2H_3O_2^{-}$	CaL^{+}	1.2
Gluconate	$C_6H_{11}O_7^{-}$	CaL_2	1.21
Glutamate	$C_5H_7NO_4^{2-}$	CaL	2.1
Phthalate	$C_8H_4O_4^{2-}$	CaL	2.4
Oxalate	$C_2O_4^{2-}$	CaL	3.2
IDA	$C_4H_5NO_4^{2-}$	CaL	3.5
Picolinate	$C_6H_4NO_2^{-}$	CaL^{+}	2.2
		CaL_2	3.8
NTA	$N_6H_6NO_6^{3-}$	CaL^{-}	7.6
Citrate	$C_6H_5O_7^{3-}$	CaL^{-}	4.7
		CaHL	9.5
		CaH_2L^{+}	12.3
EDTA	$C_{10}H_{12}N_2O_8^{4-}$	CaL^{2-}	12.4
		$CaHL^{-}$	16

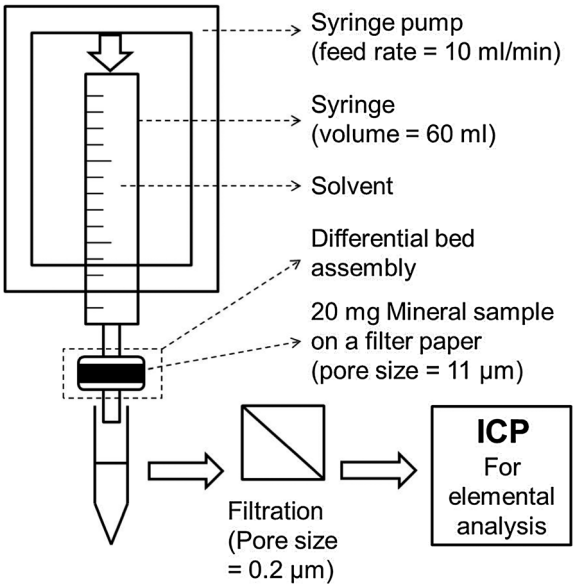

Fig. 1 schematic diagram of a differential bed reactor setup for mineral dissolution.

A small amount of wollastonite (20 mg) was uniformly distributed in a sample holder, which was then attached to the tip of the syringe containing the selected solvent. Even distribution of the mineral sample was verified for each experimental run to avoid any by-passing solvent flow. The flow rate of the solvent ($Q_{solvent}$) was set to 10 ml min^{-1}. All the experiments were performed at 295 K and the total reaction time was 6 minutes for each experimental run. The liquid samples were collected at time intervals of 8–40 seconds and re-filtered (pore size: 0.2 μm) to avoid any residual mineral particles. The liquid sample was then analyzed for elemental composition by employing an Inductively Coupled Plasma Optical Emission (ICP-OES) Spectrometer (ACTIVA-M, Horiba Jobin Yvon Inc., Edison, NJ). The chelating agents with most enhancements as well as sufficient solubilities were selected for further dissolution experiments at higher ligand concentrations.

PCC synthesis

Wollastonite was dissolved in a batch reactor using 1 M acetic acid, the slurry was filtered and the Ca-rich liquid solution was collected. The Ca-rich solution was diluted to obtain the Ca concentration of 0.5 M. The pH of the prepared Ca-rich solution (100 ml) was adjusted to match the pH of 0.5 M $Ca(NO_3)_2$ solution by dropwise adding 1 M nitric acid. The Ca-rich solution was then added to 200 ml of 0.25 M K_2CO_3 solution and stirred at 800 rpm for 30 minutes to promote the precipitation of $CaCO_3$. These carbonation experiments were performed at 295 K and 355 K to investigate the temperature effect on the particle size and the morphological structure of the produced $CaCO_3$. PCC was also produced *via* the same experimental procedure but using $Ca(NO_3)_2$ solution as a Ca^{2+} source and this model sample was used to compare PCC derived from wollastonite. For all model and wollastonite cases, the mixture was mixed at 800 rpm throughout the experiments, and the particle samples were periodically collected to determine the particle size distribution as a function of time. At the end of the carbonation experiment, the slurry was filtered and the filter cake was washed with deionized water to remove any residual chemicals. The final products, fine white powders, were obtained after drying overnight at 295 K. The produced PCC samples were then analyzed for their chemical compositions, particle sizes and morphological structures by using a battery of analytical tools including XRD, laser diffraction, Scanning Electron Microscopy (SEM, JSM-5600 LV, JEOL Ltd., Tokyo, Japan).

Results and discussion

In order to enhance the mineral carbonation and to understand each reaction step better, in this study a two-step pH swing process for wollastonite was designed and investigated: (i) wollastonite dissolution and (ii) formation of PCC. The procured wollastonite sample was ground and sieved to collect particles smaller than 175 μm. The mean particle size of the wollastonite sample was found to be 108.59 μm. By nature, procured mineral samples generally contain more than one mineral species, and thus, it was important to analyze the chemical composition and crystal structure of the prepared wollastonite sample prior to the mineral dissolution study. The chemical structure of wollastonite particles was determined by employing X-ray diffraction spectroscopy and the powder XRD pattern with Rietveld refinement fits is shown in Fig. 2. The ground powder mainly contains wollastonite (wollastonite 1A, space group: $P\bar{1}$, a = 7.963 Å, b = 7.350 Å, c = 7.034 Å, α = 90.73°, β = 95.10°, γ = 104.92°) with small amounts of wollastonite 2M (parawollastonite, space group: $P2_1$, a = 15.409 Å, b = 7.322 Å, c = 7.063 Å, β = 95.30°) and quartz. The morphological structure of wollastonite shows that ground wollastonite particles were in an irregular sheet-like shape and that their broken edges were very sharp. The elemental analysis performed using the ICP-OES *via* the lithium metaborate–acid dissolution procedure

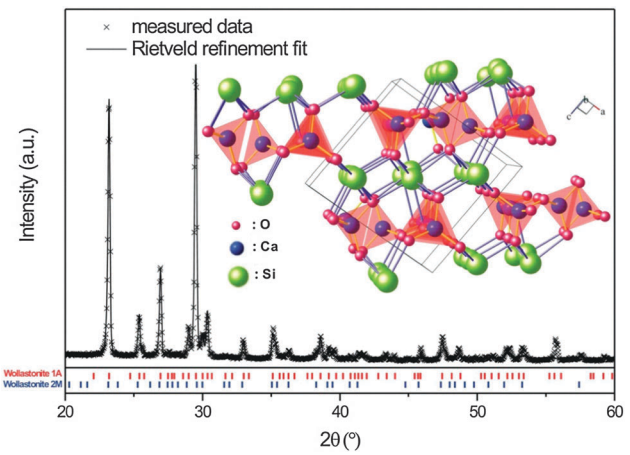

Fig. 2 XRD pattern of wollastonite and its Rietveld refined fits (R_{wp} = 14.1%). The inset illustrates the crystal structure of wollastonite 1A.

revealed that the elemental concentration of Ca was 27.0 wt% in the wollastonite mineral sample.[43]

Effects of pH and Ca-targeting ligands on wollastonite dissolution

In order to investigate the effect of chelating agents on the dissolution of wollastonite, various chelating agents were selected as listed in Table 1. Each chelating agent forms complex(s) and in some cases they may be precipitated out during its interaction with Ca^{2+} ions in solution. The reaction between the metal ion and a ligand can be expressed as,

$$mM^{x+} + lL^{y-} + hH^{+} \leftrightarrow M_m{}^{x+}\,L_l{}^{y-}H_h{}^{+} \qquad (1)$$

where M^{x+} and L^{y-} represent metal ion and ligand species, respectively. The stability constants $\left(\beta = \frac{[M_m{}^{x+}L_l{}^{y-}H_h{}^{+}]}{[M^{x+}]^m[L^{y-}]^l[H^{+}]^h}\right)$ listed in Table 1 indicate how strong these interactions would be for each set of Ca and L. As shown in reaction (1), the pH of the liquid phase plays an important role in the Ca and ligand interaction as well as the activity of the ligand varies significantly with the pH. Since it is difficult to precisely match the activities of all chelating agents in mineral slurry systems, the mineral dissolution experiments were first performed under similar pH conditions. In order to control the pH, the concentration of each chelating agent was adjusted to 0.006 M, 0.003 M, 0.002 M, and 0.0015 M for monoprotic, diprotic, triprotic, and tetraprotic acid, respectively.

Fig. 3 shows the accumulated Ca extraction (%) from wollastonite during the 6 min mineral dissolution study. A rapid mineral dissolution was observed in the first few seconds, which was mainly due to the dissolution of very fine particles (<5 μm). Fine particles have a very high surface area available for dissolution compared to larger particles. Thus, their dissolution rate are often much faster than the normal surface dissolution rate. The reaction time for the dissolution experiments was kept relatively short at 6 minutes because a longer dissolution period resulted in the formation of a passivation layer on the surface of the silicate mineral particles. Once the passivation layer was formed, the dissolution kinetic was dominated by the mass transfer through the layer rather than the surface mineral dissolution. The Ca extraction (%) for each chelating agent was calculated using the following equation,

$$\text{Ca extraction}\,(\%) = \frac{M_\mathrm{d}}{M_\mathrm{m}} \times 100 \qquad (2)$$

where M_d and M_m represent the total dissolved calcium including free Ca^{2+} ions and complexed Ca species, and the total initial amount of calcium in the starting material, respectively. Since there are twelve data series in Fig. 3, it looks relatively busy, and thus, the legend was organized in the order of the highest (0.006 M acetic acid) to the lowest (deionized water) dissolution rates. It is clear from Fig. 3 that calcium extraction from wollastonite was significantly enhanced in the presence of all chelating agents except oxalic acid. This is a particularly interesting result, since oxalic acid has been reported as one of the best chelating agents for the dissolution of Mg-bearing minerals for the purpose of carbon mineralization. In other words, it is very important to select the best ligand for each mineral. Another important point to be discussed for the data presented in Fig. 3 is that the trend in the extent of Ca extraction does not follow the order of the stability constants.

Fig. 4, which was prepared based on the data given in Fig. 3 at 6 minutes and the initial pHs of the solvents, more clearly illustrates the effect of chelating agents on wollastonite dissolution. Except for the deionized water, the pH of most solvents ranged from 2.5 to 4. Calcium extraction is generally enhanced under lower pH conditions. Interestingly, the solvent containing 0.003 M oxalic acid, which shows a pH of ~2.6, exhibited the lowest Ca extraction (%) among studied chelating agents. While the stability constant of the Ca–oxalate complex was not the lowest of all the chelating agents tested, oxalic acid was found

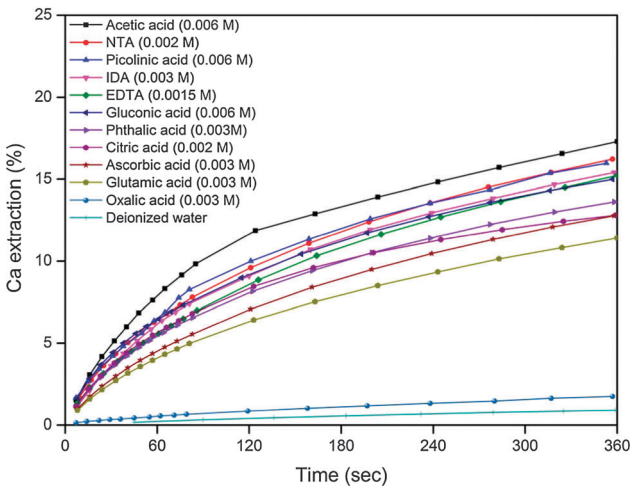

Fig. 3 The effect of various chelating agents on Ca extraction from wollastonite as a function of time (reaction time = 6 min, temperature = 295 K, $Q_{solvent}$ = 10 ml min^{-1}).

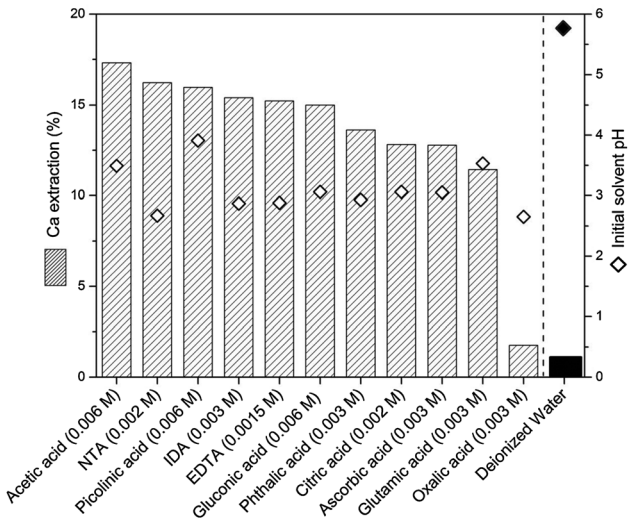

Fig. 4 Comparison of Ca extraction from wollastonite using various chelating agents (reaction time = 6 min, temperature = 295 K, $Q_{solvent}$ = 10 ml min^{-1}).

to be inefficient for enhancing the wollastonite dissolution because the solubility of calcium oxalate is very low (0.000052 M at 293 K). Calcium oxalate precipitated out during the dissolution of wollastonite, and therefore, the overall extent of Ca extraction was limited. Other chelating agents performed quite well in accelerating the wollastonite dissolution. Chelating agents such as acetic acid, NTA and picolinic acid, significantly enhanced the Ca extraction from wollastonite reaching as high as 17.4% in 6 minutes. This is again interesting since their initial solvent pH values were not the lowest among the studied solvents. The initial pHs of those two solvents were ~3.5 (acetic acid) and ~3.9 (picolinic acid).

The activity of each chelating agent in the aqueous solution depends on the system pH. Each chelating agent/ligand can make one or several complexes with Ca^{2+} as well as a proton, and each complex possesses a different stability constant.[44] In order to investigate the activity of each chelating agent under different pH conditions, the activities of the four main chelating agents studied (*i.e.*, acetate, oxalate, citrate and $EDTA^{4-}$) were simulated as a function of pH using the thermodynamic calculation software (*i.e.*, Visual MINTEQ). As shown in Fig. 5, while $EDTA^{4-}$ can form the most stable complexes with Ca, its activity at a pH of 2.8 was very low. On the other hand, acetate has a relatively low stability constant for its complex with Ca, but its activity at a pH of 3.5 was considerably higher than that of $EDTA^{4-}$. In the case of oxalate, both the stability constant and the activity at the initial solvent pH were competitive, but because of the extremely low solubility of the produced Ca–oxalate complex, oxalate's performance in enhancing wollastonite dissolution was not as effective as other ligands'. As mentioned earlier, the system pH was different for each chelating agent because the acidic forms of chelating agents were used without buffering the solution.

Based on the wollastonite dissolution results and considering the solubility of each chelating agent, three chelating agents, gluconate, citrate and acetate, were selected for further study.

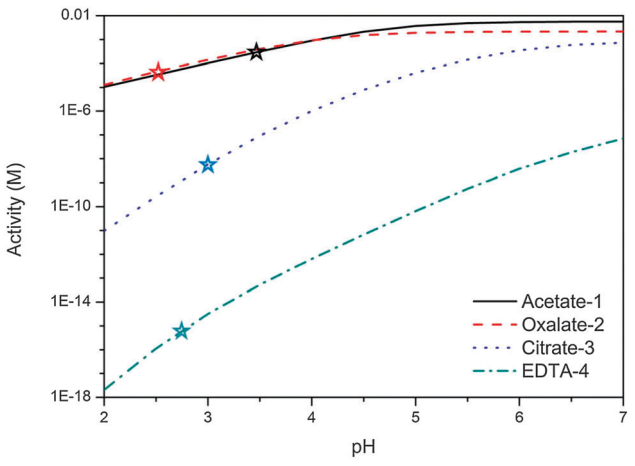

Fig. 5 Simulation results of the activities of chelating agents as a function of pH obtained using Visual MINTEQ. (Concentrations of acetate, oxalate, citrate and EDTA were 0.006 M, 0.003 M, 0.002 M and 0.0015 M, respectively. Stars mark the measured initial pH values of the solvents used in the experimental studies.)

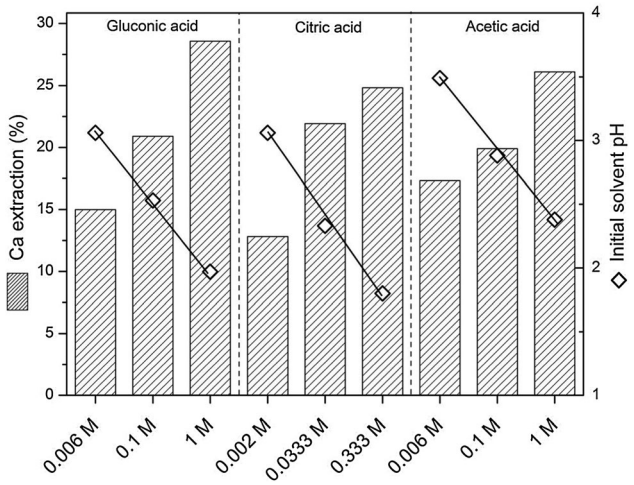

Fig. 6 The effect of chelating agent concentrations on Ca extraction from wollastonite (reaction time = 6 min, temperature = 295 K, $Q_{solvent}$ = 10 ml min^{-1}). Note that in order to keep the similar pH levels throughout the experiments, the concentrations of citric acid-containing solvents were lower, because citric acid is a triprotic acid, whereas the other two chelating agents are monoprotic acids.

In order to optimize the wollastonite dissolution step, higher concentrations of these ligands were tested and the results are shown in Fig. 6. As expected, the Ca extractions (%) were significantly increased as the concentration of the chelating agents was increased. These results were also confirmed by batch mineral dissolution experiments. It was found that compared to the kinetic studies performed using the differential bed reactor which was operated far from the equilibrium, the batch mineral dissolution was limited by the solubility of Ca–ligand complexes, particularly for the citrate case (low solubility of <1 g l^{-1} at 25 °C if the system pH is higher than 7).

Synthesis of morphologically controlled PCC

The $CaCO_3$ particles synthesized from two different Ca sources, wollastonite and $Ca(NO_3)_2$, were compared to investigate the effect of heterogeneity of wollastonite on the PCC formation. Fig. 7 shows the particle size distributions of $CaCO_3$(W) and $CaCO_3$(M) at two different temperatures of 295 K and 355 K. As shown in Fig. 7, their particle size distributions at 295 K were similar, whereas their particle size distributions at 355 K were quite different. It has been reported in the literature that the organic additives and surface modifiers could affect the morphological structure of PCC.[45,46] Thus, the differences could be attributed to the use of acetic acid to extract Ca from wollastonite. The presence of other ionic species leached out from wollastonite along with calcium could also affect the formation and the quality of PCC. XRD patterns of $CaCO_3$(W) and $CaCO_3$(M) samples were also analyzed to determine the crystalline structures and compositions of synthesized PCC. The XRD patterns of $CaCO_3$(W) and $CaCO_3$(M) synthesized at 297 K and 355 K, and their Rietveld refinement fits are given in Fig. 8. The XRD analyses show that both $CaCO_3$(W) and $CaCO_3$(M) produced at 295 K contained two different crystalline structures of PCC: vaterite (space group: $P6_3/mmc$, a = 4.12 Å,

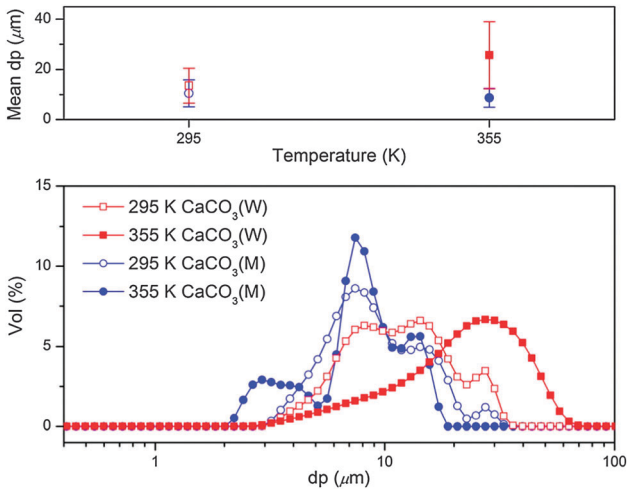

Fig. 7 Comparison of mean particle sizes (top) and particle size distributions (bottom) of $CaCO_3$ synthesized using Ca-rich solutions derived from wollastonite and $Ca(NO_3)_2$ at 295 K and 355 K (reaction time = 30 min, stirring rate = 800 rpm).

c = 8.45 Å) and calcite (space group: $R\bar{3}c$, a = 4.99 Å, c = 17.05 Å). In the case of $CaCO_3$(W), it contained 24 wt% of calcite and 76 wt% of vaterite, whereas the fraction of calcite and vaterite in $CaCO_3$(M) were 33 wt% and 67 wt%, respectively. Vaterite is metastable, it is not only less common in nature but also commercially a less significant polymorph of PCC. In contrast, calcite is the most common polymorph of PCC used in commercial applications. At the higher temperature of 355 K (Fig. 8(b)), both produced $CaCO_3$(W) and $CaCO_3$(M) changed their polymorphic structures to aragonite (space group: *Pnma*, a = 4.95 Å, b = 7.96 Å, c = 5.74 Å) with a small amount of calcite ($CaCO_3$(W): 87 wt% of aragonite with 13 wt% of calcite, $CaCO_3$(M): 96 wt% of aragonite with 4 wt% of calcite). Aragonite was observed as a major polymorph of $CaCO_3$ at 355 K because a phase transition from vaterite to aragonite occurs at above 330 K.[47]

Fig. 9 shows a comparison of the morphological structures of $CaCO_3$(W) synthesized at 295 K and 355 K with their corresponding $CaCO_3$(M) structures. As shown in Fig. 9(a) and (b), PCC particles synthesized at 295 K exhibited spherical shapes, but the shape of the formed PCC changed to needle-like at a higher reaction temperature (Fig. 9(c) and (d)). Generally aragonite exhibits needle-shaped orthorhombic structures, and the aspect ratio (length-to-diameter) is a very important property in many applications, particularly for aragonite. The high aspect ratio of aragonite is suitable for the applications that require high strength and incident light scattering. While the general trend in the morphological changes as a function of reaction temperature was similar for $CaCO_3$(W) and $CaCO_3$(M), it was observed that PCC synthesized from Ca-rich solution derived from wollastonite was larger and more irregular in its shape. Thus, for the ultimate use of PCC produced *via* enhanced carbonation of wollastonite the particle size and the morphological structures can be tuned for specific application (*e.g.*, paper fillers, construction materials).

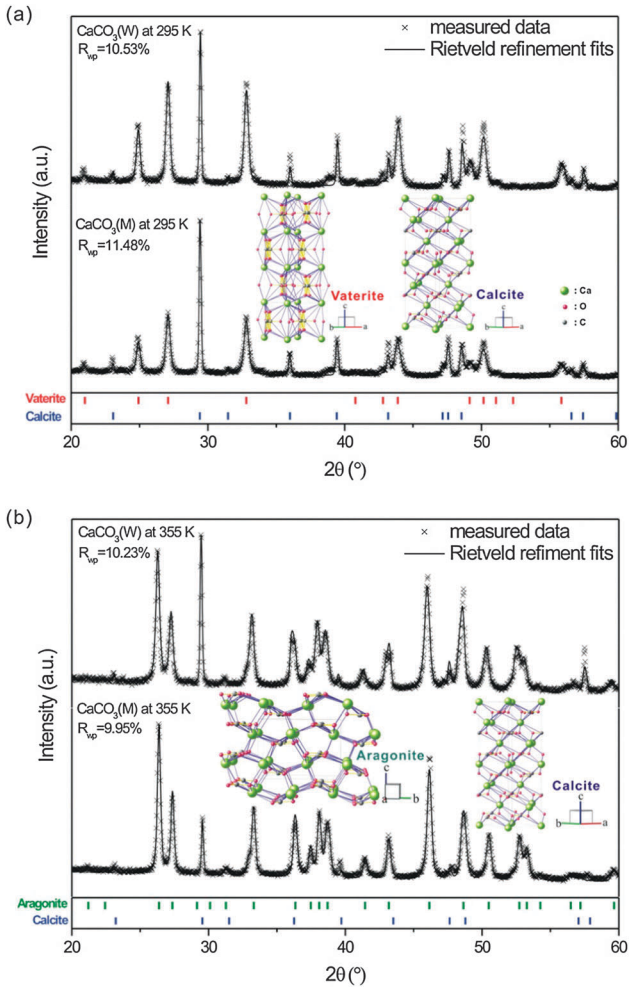

Fig. 8 XRD patterns and their Rietveld fits for $CaCO_3$ synthesized using Ca-rich solutions derived from wollastonite and $Ca(NO_3)_2$ at (a) 295 K and (b) 355 K. Insets indicate the crystalline structures of vaterite, calcite and aragonite.

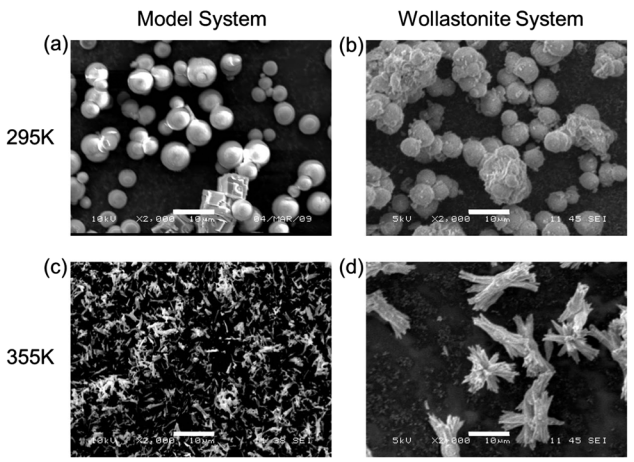

Fig. 9 SEM images of $CaCO_3$ synthesized using Ca-rich solution derived from the model system of $Ca(NO_3)_2$ ((a) and (c)) and wollastonite ((b) and (d)) under two temperature conditions of 295 K and 355 K. The scale bars in SEM images are all in the length of 10 μm.

Conclusion

In this study, the enhanced carbonation of Ca-bearing mineral (*i.e.*, wollastonite) was systematically investigated in two separate steps. In the first mineral dissolution step, various chelating agents were selected and studied to accelerate the leaching of Ca from wollastonite. The effects of both the type of chelating agents and their concentrations were investigated and the results were discussed along with the effect of the solvent pH. It was found that all the chelating agents tested in this study enhanced the dissolution of wollastonite. Interestingly, oxalate which has been reported in the literature as one of the best chemical additives for the magnesium silicate minerals did not significantly accelerate the dissolution of wollastonite. This illustrates that the mineral dissolution solvent containing chelating agents should be prepared carefully considering the mineralogy of each geologic formation. After the dissolution of wollastonite, the leached Ca was reacted with a carbonate solution to form PCC. This study showed that by controlling the reaction temperature, the morphological structure of the synthesized PCC can be tuned for various applications (*i.e.*, paper fillers, plastic fillers and construction materials). It was also found that the presence of chelating agents resulted in the changes of the particle size and shape during the synthesis of PCC.

Acknowledgements

The work presented in this paper was partially funded by New York State Energy Research and Development Authority (Agreement Number 10144), National Science Foundation and U.S. Department of Energy.

References

1 IPCC, *Climate Change 2007: Synthesis Report*, Cambridge Univ. Press, New York, 2007.
2 IPCC, *Carbon Dioxide Capture and Storage*, Cambridge Univ. Press, New York, 2005.
3 IEA, *World Energy Outlook 2010*, Organization for Economic Co-operation and Development, 2010.
4 K. S. Lackner, A guide to CO_2 sequestration, *Science*, 2003, **300**, 1677–1678.
5 R. S. Haszeldine, Carbon capture and storage: how green can back be? *Science*, 2009, **325**, 1647–1652.
6 S. Holloway, Storage of fossil fuel-derived carbon dioxide beneath the surface of the earth, *Annu. Rev. Energy*, 2001, **26**, 145–166.
7 F. M. Orr Jr., Onshore geologic storage of CO_2, *Science*, 2009, **325**, 1656–1658.
8 P. G. Brewer, G. Friederich, E. T. Pelzer and F. M. Orr. Jr., Direct experiments on the ocean disposal of fossil fuel CO_2, *Science*, 1999, **284**, 943–945.
9 J. H. Martin, K. H. Coale, K. S. Johnson, S. Fitzwater, R. M. Gordon, S. J. Tanner, C. N. Hunter, V. A. Elrod, J. L. Nowickl, T. L. Coley, R. T. Barber, S. Lindley, A. J. Watson, K. van Scoy, C. S. Law, M. I. Liddicoat, R. Ling, T. Stanton, J. Stockel, C. Collins, A. Anderson, R. Bidigare, M. Ondrusek, M. Latasa, F. J. Millero, K. Lee, W. Yao, J. Z. Zhang, G. Freiderich, C. Sakamoto, F. Chavez, K. Buck, Z. Kolber, R. Greene, P. Falkowski, S. W. Chisholm, F. Hoge, R. Swift, J. Yungel, S. Turner, P. Nightingale, A. Hatton, P. Liss and N. W. Tindale, Testing the iron hypothesis in ecosystems of the equatorial Pacific Ocean, *Nature*, 1994, **371**, 123–129.
10 W. Seifritz, CO_2 disposal by means of silicates, *Nature*, 1990, **345**, 486.
11 L.-S. Fan, A.-H. A. Park and K. S. Lackner, Carbon dioxide capture and disposal: carbon sequestration, in *Encyclopedia of Chemical Processing*, ed. S. Lee, CRC Press, Boca Raton, FL, 2005, p. 305.
12 A.-H. A. Park, K. S. Lackner and L.-S. Fan, Carbon sequestration, in *Hydrogen Fuel: Production, Transport and Storage*, ed. R. Gupta, CRC Press, Boca Raton, FL, 2008, p. 569.
13 R. Zevenhoven and J. Fagerlund, Fixation of CO_2 into inorganic carbonates: the natural and artificial ''weathering of silicates'', in *Carbon Dioxide as Chemical Feedstock*, ed. M. Aresta, Wiley VCH Verlag, Germany, 2010, p. 353.
14 T. Kojima, A. Nagamine and S. Uemiya, Absorption and fixation of carbon dioxide by rock weathering, *Energy Convers. Manage.*, 1997, **34**, 461–466.
15 W. D. Gunter, E. H. Perkins and T. J. McCann, Aquifer disposal of CO_2 rich gases: reaction design for added capacity, *Energy Convers. Manage.*, 1993, **34**, 941–948.
16 D. P. Butt, K. S. Lackner, C. H. Wendt, R. Vaidya, L. Piled, Y. Park, T. Holesinger, D. M. Harradine, K. Nomura, The kinetics of binding carbon dioxide in magnesium carbonate, Proceedings of the 23rd International Technical Conference on Coal Utilization and Fuel Systems, Clearwater, FL, 1998.
17 K. S. Lackner, D. P. Butt and C. H. Wendt, Progress on binding CO_2 in mineral substrates, *Energy Convers. Manage.*, 1997, **38**, 259–264.
18 P. S. Newall, S. J. Clarke, H. M. Haywood, H. Scholes, N. R. Clarke, P. A. King and R. W. Barley, *CO_2 storage as carbonate minerals, Report number PH3/17,* IEA Greenhouse Gas R&D Programme, 2000.
19 R. Zevenhoven, J. Fagerlund and J. K. Songok, CO_2 mineral sequestration: developments toward large-scale application, *Greenhouse Gases: Sci. Technol.*, 2011, **1**, 48–57.
20 W. K. O'Connor, D. C. Dahlin, D. N. Nilsen, R. P. Walters, P. C. Turner, Carbon dioxide sequestration by direct mineral carbonation with carbonic acid, Proceedings of the 23rd International Technical Conference on Coal Utilization and Fuel Systems, Clearwater, FL, 1998.
21 W. K. O'Connor, D. C. Dahlin, G. E. Rush, S. J. Gerdemann, L. R. Penner and R. P. Nilsen, *Aqueous Mineral Carbonation: Mineral Availability, Pretreatment, Reaction Parametrics, and Process Studies*, DOE/ARC-TR-04-002, Albany Research Center, Albany, OR, 2005.
22 S. J. Gerdemann, W. K. O'Connor, D. C. Dahlin, L. R. Penner and H. Rush, Ex situ aqueous mineral carbonation, *Environ. Sci. Technol.*, 2007, **41**, 2587–2593.

23 M. Hanchen, V. Prigiobbe, G. Storti, T. M. Seward and M. Mazzotti, Dissolution kinetics of fosteritic olivine at 90–150 °C including effects of the presence of CO_2, *Geochim. Cosmochim. Acta*, 2006, **70**, 4403–4416.
24 M. Hanchen, S. Krevor, M. Mazzotti and K. Lackner, Validation of a population balance model for olivine, *Chem. Eng. Sci.*, 2007, **62**, 6412–6422.
25 M. Kakizawa, A. Yamasaki and Y. Yanagisawa, A new CO_2 disposal process *via* artificial weathering of calcium silicate accelerated by acetic acid, *Energy*, 2001, **26**, 341–354.
26 A.-H. A. Park and L. Fan, CO_2 mineral sequestration: physically activated dissolution of serpentine and pH swing process, *Chem. Eng. Sci.*, 2004, **59**, 5241–5247.
27 M. M. Maroto-Valer, D. J. Fauth, M. E. Kuchta, Y. Zhang and J. M. Andresen, Activation of magnesium rich minerals as carbonation feedstock materials for CO_2 sequestration, *Fuel Process. Technol.*, 2005, **86**, 1627–1645.
28 K. Jarvis, R. W. Carpenter, R. Windman, Y. Kim, R. Nunez and F. Alawneh, Reaction mechanism for enhancing mineral sequestration of CO_2, *Environ. Sci. Technol.*, 2009, **43**, 6314–6319.
29 S. C. Krevor and K. S. Lackner, Enhancing process kinetics for mineral carbon sequestration, *Energy Procedia*, 2009, **1**, 4867–4871.
30 S. C. Krevor and K. S. Lackner, Enhancing serpentine dissolution kinetics for mineral carbon dioxide sequestration, *Int. J. Greenhouse Gas Control*, 2011, **5**, 1073–1080.
31 O. S. Pokrovsky, L. S. Shirokova, P. Benezeth, J. Schott and S. V. Golubev, Effect of organic ligands and heterotrophic bacteria on wollastonite dissolution kinetics, *Am. J. Sci.*, 2009, **309**, 731–772.
32 V. Prigiobbe, M. Hanchen, M. Werner, R. Baciocchi and M. Mazzotti, Mineral carbonation process for CO_2 sequestration, *Energy Procedia*, 2009, **1**, 4885–4890.
33 F. Goff and K. S. Lackner, Carbon dioxide sequestering using ultramafic rocks, *Environ. Geosci.*, 1998, **5**, 89–101.
34 E. H. Oelkers, S. R. Gislason and J. Matter, Mineral carbonation of CO_2, *Elements*, 2008, **4**, 333–337.
35 S. Teir, S. Eloneva, C. J. Fogelholm and R. Zevenhoven, Dissolution of steelmaking slags in acetic acid for precipitated calcium carbonate production, *Energy*, 2007, **32**, 528–539.
36 D. A. Singer and W. D. Menzie, *Quantitative mineral resource assessments – an integrated approach*, Oxford University Press, Oxford, U.K., 2010.
37 U.S. Geological Survey, *Mineral Commodity Summaries*, January 2011.
38 W. J. J. Huijgen, G. J. Witkamp and R. N. J. Comans, Mineral CO_2 sequestration by steel slag carbonation, *Environ. Sci. Technol.*, 2005, **39**, 9676–9682.
39 A. Iizuka, M. Fujii, A. Yamasaki and Y. Yanagisawa, Development of a new CO_2 sequestration process utilizing the carbonation of waste cement, *Ind. Eng. Chem. Res.*, 2004, **43**, 7880–7887.
40 D. N. Huntzinger, J. S. Gierke, S. K. Kawatra, T. C. Eisele and L. L. Sutter, Carbon dioxide sequestration in cement kiln dust through mineral carbonation, *Environ. Sci. Technol.*, 2009, **43**, 1986–1992.
41 S. Teir, S. Eloneva and R. Zevenhoven, Production of precipitated calcium carbonate from calcium silicates and carbon dioxide, *Energy Convers. Manage.*, 2005, **46**, 2954–2979.
42 L. Lutterotti, S. Matthies, H.-R. Wenk, A. S. Schultz and J. W. Richardson, Combined texture and structure analysis of deformed limestone from time-of-flight neutron diffraction spectra, *J. Appl. Phys.*, 1997, **81**, 594–600.
43 C. Feldman, Behavior of trace refractory minerals in the lithium metaborate fusion-acid dissolution procedure, *Anal. Chem.*, 1983, **55**(14), 2451–2453.
44 M. Gajewski and M. Klobukowski, DFT studies of complexes between ethylenediamine tetraacetate and alkali and alkaline earth cations, *Can. J. Chem.*, 2009, **87**, 1492–1498.
45 R. Agnihotri, S. K. Mahuli, S. S. Chauk and L.-S. Fan, Influence of surface modifiers on the structure of precipitated calcium carbonate, *Ind. Eng. Chem. Res.*, 1999, **38**, 2283–2291.
46 W. K. Park, S.-J. Ko, S. W. Lee, K.-H. Cho, J.-W. Ahn and C. Han, Effects of magnesium chloride and organic additives on the synthesis of aragonite precipitated calcium carbonate, *J. Cryst. Growth*, 2008, **310**, 2593–2601.
47 K. Fuchigami, Y. Taguchi and M. Tanaka, Synthesis of calcium carbonate vaterite crystals and their effect on stabilization of suspension polymerization of MMA, *Adv. Powder Technol.*, 2009, **20**, 74–79.

